Static / dynamic trade-off performance of PZT thickfilm micro-actuators

Alex Bienaimé, Vincent Chalvet, Cédric Clévy, Ludovic Gauthier-Manuel, Thomas Baron and Micky Rakotondrabe

FEMTO-ST Institute, AS2M department,
Université de Franche-Comté/CNRS/ENSMM/UTBM,
24 rue Savary, 25000 Besançon, France.

E-mail: vincent.chalvet@femto-st.fr, cclevy@femto-st.fr, mrakoton@femto-st.fr

Abstract. Piezoelectric actuators are widespread for the design of micro/nanorobotic tools and microsystems. Studies toward the integration of such actuators in complex micromechatronic systems require the size reduction of these actuators with a large range of performances. Two main fabrication processes are nowadays used for the fabrication of piezoelectric actuators, providing very different behaviors: i) the use of bulk PZT layer, ii) and the use of thin film growth. In this paper, we propose a trade-off between these tow extremes processes and technologies in order to explore new actuators performances. It resulted in the design and fabrication of thick film PZT unimorph cantilevers. They allowed the generation of high performances, both in the static (displacement) and dynamic (first resonance frequency) regimes, in addition to the small sizes. Such cantilevers size are obtained through the wafer scale bonding and thinning of PZT plate onto a SOI wafer. The piezoelectric cantilevers have a PZT layer of 26 µm thickness with a 5 µm thick silicon layer, over a length of 4 mm and a width of 150 µm. The experimental characterization has shown that the static displacements obtained are in excess of $4.8\,\mu m\,V^{-1}$ and the resonance frequency up to 1103 Hz, which are useful for large displacements and low voltage actuators.

1. Introduction

Miniaturized systems are more and more present in different applications in our everyday's life. These last years, such systems became smaller, smarter, with better performances and more customization which results in an increasing density of functionalities. The related industrial potential is huge and covers a wide range of applications in very different fields such as energy [1], biology [2], medicine [3], instrumentation [4] and robotics [5], for instance: Optical Coherence Tomography for endoscopes or mini-invasive surgery, energy harvesting, micro-assembly, cell characterization, microspectrometers, implantable optical sensors, optical interconnects, photon counters, etc. This tendency is notably supported by the increasing possibility of clean room microfabrication techniques, integration of active materials and designs based on compliant structures [5, 6]. Nevertheless, the main challenge is the integration of different physical components in such a miniaturized system while allowing highly efficient

behavior: for example a large range of motion/deformation, high bandwidth, high stiffness, high resolution, small sizes, low energy consumption, and sensing possibility with the same actuator. Therefore, for such purpose, piezoelectric smart materials are widely used for the design of miniaturized systems thanks to their ability to satisfy most of these requirements [7] and to their easy manufacturability. One of the most utilized structures of piezoelectric systems is the piezoelectric bender which has a cantilever structure. For instance, it can be utilized as actuator in scanning probe microscopes [8], precise and highly dynamic positioners in micromanipulation and microassembly [9] or actuators for laser scanning in medical applications [10]. Alternatively sensor applications are also concerned, leading to promising sensing studies in the domain of mass detection [11, 12] , biosensors [13, 14, 15, 16, 17], and even microscale force sensors [18]. Similar technologies are employed for the design of these sensing microsystems, but appear with different shapes and sizes, not only cantilevers.

There are two main ways to fabricate piezoelectric benders:

(i) a bulk approach which enables to have thick actuators (typically more than 200 µm thickness) providing a high inherent stiffness, good dynamics (kHz frequencies range), but small output displacements (typically some tens of µm). The thicknesses of the actuators are such that high voltages (some hundreds of volts) are required to reach the expected displacements. Therefore, to maximize the displacements, the length of the actuator is often increased (in the design step) resulting in quite bulky devices (tens of mm long beam).

(ii) a thin film approach consisting of the deposition of thin layers of piezoelectric materials (typically in the range of some µm). This approach enables the fabrication of very small actuators (often much smaller than a mm). Since the thicknesses are very small, high electrical fields are obtained for the same range of driving voltages as in bulk. Consequently, the fabricated actuators can reach very large displacements (hundreds of µm) with low voltages. Nevertheless, the stiffness obtained with this approach is low which makes it not efficient for actuations that require high torque. Furthermore, the structures are typified by very low dynamics (much less than a kHz).

These two main approaches enable the fabrication of performant actuators but with very different features [19]. There is therefore a high interest to succeed in the fabrication of intermediate structures, relying on "thick film" piezoelectric layers, with thicknesses ranging between 5 and 150 µm, enabling the combination of several interesting performances taken from both thin film (large motions, low voltage, small sizes) and bulk properties (high stiffness and torque, high dynamics). The literature shows different approaches to investigate thick film fabrication, see for instance the survey in [20]. They can be classified into growing techniques (sputtering, chemical solution, deposition or evaporation) [21], and into subtractive techniques (bulk micromachining with for example wet etching, dry etching). Growing techniques usually enable the realization of films up to 25 µm thicknesses. However, it is difficult to control the crystallography and, therefore, the film properties. As a result, such thick films exhibit a similar performance as thin films. On the other hand, subtractive techniques usually

consist of bonding a bulk piezoelectric ceramic onto a substrate (passive or active too) and afterwards thinning the bonded piezoelectric layer. This thinning can either be achieved by wet etching or mechanical thinning. By using wet etching the control of the piezoelectric layer thickness remains a difficult task. In addition, the etched surface shows less performance than conventional bulk material. Mechanical thinning is relatively easy to achieve but the initial bonding of the piezo layer is usually performed at high temperature (up to 550°C [22, 23, 24]). Such high temperatures being over the Curie temperature of the piezoelectric material (which is 230°C in our case) results in the depolarization of the piezoelectric layer. An additional re-polarization step is then required. As explained in [1], a safe functioning temperature is about half way between 0°C and the Curie point. For this reason several studies [1, 25, 26] contributed to reduce the temperature bonding down to $110 \sim 200$°C. However, during the thermocompression bonding process, the difference of thermal dilatation between PZT and silicon (as small as it is) results in residual mechanical stress. This is particularly the case for wafer scale bonding as done here.

In this paper we investigate the fabrication of thick film piezoelectric cantilevers obtained by a bonding process at room temperature (~ 20°C) and mechanical thinning of the piezoelectric layer. The aim of this approach is to obtain piezoelectrically actuated structures with low remaining mechanical stress and with very high performances benefit from both bulk properties and thin films properties. Different cantilevers sizes are designed, generating a wide range of performances. Such active structures are essential for integration in complex systems where small sizes and good performances are required.

The remainder of this article is organized as follows. Section-2 provides a performance analysis of unimorph piezoelectric cantilever actuators (chosen as a case of study due to its genericity and widespread use) versus the design parameters. The objective of the analytical linear model is to provide an understanding of the device performance as function of some essential miniaturization parameters, such as device thickness and length. Section-3 presents the microfabrication process used and the fabricated unimorphs. Their performances are experimentally quantified in section-4 to state the validity of the approach. In section-5 the conclusions of the study are presented.

2. Performances analysis of unimorph piezoelectric cantilever actuators

The unimorph cantilever is a generic structure often used as an actuation device in microsystems, then chosen in this paper as case of study. A unimorph piezoelectric cantilever is composed of two layers: one piezoelectric layer called active layer (for instance based on the lead zirconate titanate or PZT ceramic) and one passive layer, also called elastic layer, made from a non-piezoelectric material (silicon, copper, nickel, chrome for instance). In this paper, the active layer is based on bulk PZT while the passive layer is silicon. A very thin ($300\,nm$) gold layer is used as interface and bond between the silicon and the PZT. It also serves as electrode. Applying an input voltage between the gold electrode and a second electrode (also made of gold) deposited on the top surface of the PZT layer results in an extension/contraction of the piezoelectric layer, and thus in a bending displacement δ of the

overall cantilever (see Figure 1). The behavior of such cantilevers has been well studied and extrapolated to multilayer cantilevers [27]. We propose here an analysis of the performances of the cantilever according to some essential parameters of miniaturization which are the thicknesses and the lengths of the layers. The aim of the analysis is to show the significance of the approach compared to bulk PZT technology and to thin film technology.

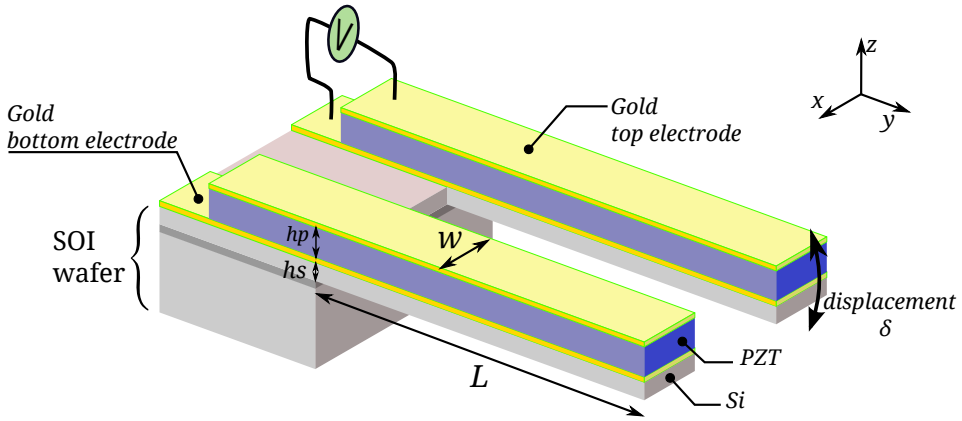

Figure 1: A unimorph piezoelectric cantilever actuator.

2.1. Theoretical behavior of a unimorph piezoelectric cantilever

From the generalized multimorph piezoelectric equation developed by Ballas in [27], the equation for a unimorph bulk PZT cantilever can be deduced. Assuming negligible thickness for the gold layer, the static bending displacement δ of the unimorph cantilever at its tip is:

$$\delta = \frac{-3d_{31}S_{11}^{s}S_{11}^{p}h_s(h_p+h_s)L^2}{(S_{11}^{p})^2h_s^4+S_{11}^{s}S_{11}^{p}(4h_ph_s^3+6h_p^2h_s^2+4h_sh_p^3)+(S_{11}^{s})^2h_p^4}\times V \quad (1)$$

whilst its first resonance frequency is:

$$f_r = \frac{1.8751^2h_p}{2\pi L^2}\times\sqrt{\frac{(S_{11}^{p})^2(\frac{h_s}{h_p})^4+S_{11}^{p}S_{11}^{s}(4(\frac{h_s}{h_p})^3+6(\frac{h_s}{h_p})^2+4\frac{h_s}{h_p})+(S_{11}^{s})^2}{12S_{11}^{s}S_{11}^{p}(S_{11}^{s}+S_{11}^{p}\frac{h_s}{h_p})(\rho_s\frac{h_s}{h_p}+\rho_p)}} \quad (2)$$

where the parameters and their numerical values are listed in Table 1. The 1.8751 coefficient in Eq. 2 corresponds to the value of a coefficient for the first mode of resonance. For higher modes, this value is different [27]. In the rest of this paper, Eq. 1 and 2 are used to analyze the behavior of a piezoelectric cantilever.

Figure 2(a) displays the theoretical displacement/voltage ratio for a cantilever of 4 mm length as a function of the PZT layer thickness (h_p). h_p varies between 0 and 250 µm to cover typical values of different types of unimorphs (from thin film to bulk). The simulations were done for four different silicon layer thicknesses (h_s = 1, 10, 50 and 100 µm). The resonance frequencies for the same cantilever dimensions are given in Figure 2(b).

Standard fabrication of cantilevers utilize bulk PZT layers (thickness $>$ 160 µm). Thin film grown PZT layers usually have a thickness less than 2 µm. The theoretical performance

Table 1: List of Variables

Variable	Definition	Value for our case	Unit
T_c	Curie temperature of the PZT-5H	230	°C
d_{31}	Piezoelectric coefficient of the PZT-5H	-320×10^{-12}	m V^{-1}
S_{11}^p	Elastic compliance at constant electric field of PZT-5H	16.13×10^{-12}	m^2/N
S_{11}^s	Elastic compliance of silicon	7.68×10^{-12}	m^2/N
ρ_p	PZT-5H density	7800	kg/m^3
ρ_s	Silicon density	2329	kg/m^3
h_p	Active layer (PZT) thickness	$0<h_p<250$	µm
h_s	Passive layer (Silicon) thickness	$0<h_s<100$	µm
L	Length of the cantilever	$0<L<200(h_p+h_s)$	µm
V	Input voltage	$-100<V<100$	V

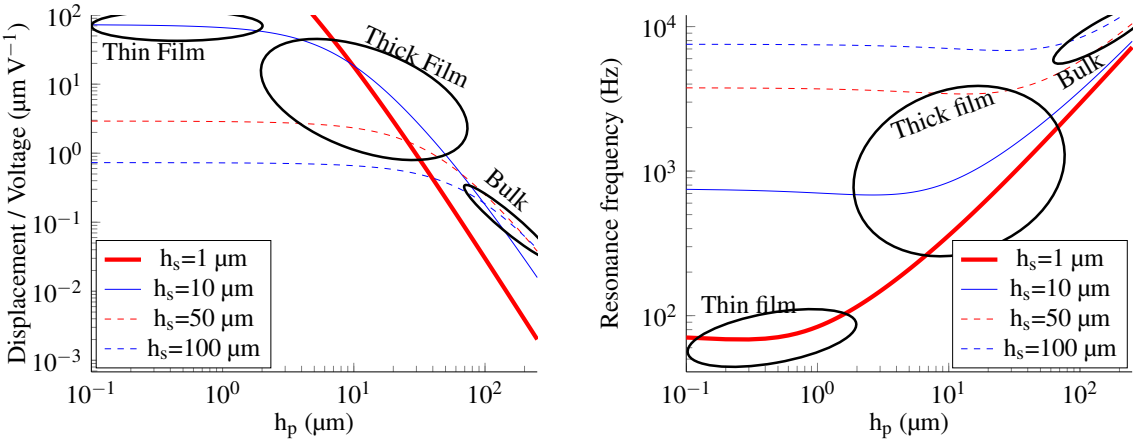

(a) (a) (b) (b)

Figure 2: Theoretical displacement (a) and first resonance frequency (b) for different kinds of unimorph cantilevers: influence of the PZT layer thickness for four silicon layer thicknesses, with a length $L=4$ mm.

of these two kinds of actuators are shown in Figure 2. These graphs show that PZT thin films allow the generation of large displacements of the cantilever. However they provide low bandwidth and low stiffness structures. In contrast bulk layers generate small displacements but have a large bandwidth and high stiffness.

The goal of this paper is to investigate a new range of piezoelectric actuators with trade-off performances both in the static and dynamic domains, inherited from the advantages of bulk and thin films. For this purpose, the thinning of the bulk PZT layer is studied, resulting in thick film PZT micro-actuators.

Table 2: List of all fabricated cantilevers.

Reference name	Long_1	Long_2	Long_3	Short_1	Short_2	Short_3
PZT thickness h_p (µm)	40	80	160	11	26	48
Si thickness h_s (µm)	50	50	50	5	5	5
cantilever length L (mm)	10	10	10	4	4	4

2.2. Design choice

The purpose of the design step is to study a representative set of cantilevers dimensions to show the obtainable trade-off of static and dynamic properties. In order to investigate the range of dimensions between the bulk PZT and the thin films, several cantilevers have been fabricated. Two sets of unimorph piezoelectric cantilevers are studied: one set with a thick silicon layer (50 µm) and the other set with a thin silicon layer (5 µm) for which the thickness of the PZT layer is reduced even more. All these cantilevers are obtained from a thinning process of the bulk PZT layer. The initial thickness (before thinning) of the bulk is 160 µm.

The two sets are fabricated from two different SOI (silicon on insulator) wafers with different device layer thicknesses. Each wafer's device layer is used as the silicon passive layer for the cantilever. One set is fabricated on a 50 µm device layer SOI wafer, and the other one uses a 5 µm thickness device layer. In order to carry out experiments with different lengths we also fabricate cantilevers of two sets of lenghts. The first one of 10 mm, and a second set of 4 mm length cantilevers. A list of these fabricated cantilevers is shown in Table 2, with their reference names that will be used further on in this paper.

3. Presentation of the microfabrication process

A critical step in the microfabrication process is the bonding of the PZT layer onto the SOI wafer. Existing processes used for the bonding and thinning of bulk PZT, employed temperatures of $110 \sim 200$°C [1, 25, 26] during the thermocompression step. In order to limit the generation of mechanical stress inside the structure, we propose here to keep the bonding step at room temperature. This is inspired from a process for bonding materials with different thermal expansion coefficients [29]. Thanks to that process, an additional repolarization step is not required, and residual mechanical stress in the designed structure is prevented.

The whole process flowchart is detailed in Figure 3. It consists of the following steps: One side of the 160 µm bulk PZT is first polished (step **1**) with colloidal silica. A thin film ($\sim 300\,nm$) of chromium-gold (Cr-Au) can then be deposited on this polished side, and also on the device layer of the SOI wafer (step **2**). The SOI wafer is composed of a 300 µm thick handle layer, a 1 µm buried oxide layer and a 5 µm device layer (or 50 µm for the one used for long cantilevers). The gold layers deposited on the two surfaces will be used for the gold bonding (step **3**) between the PZT bulk and the device layer of the SOI wafer. The two gold surfaces are put in contact and compressed together with a wafer bonder for a few minutes at room temperature. Final bonding of the two gold layers is then obtained after compression

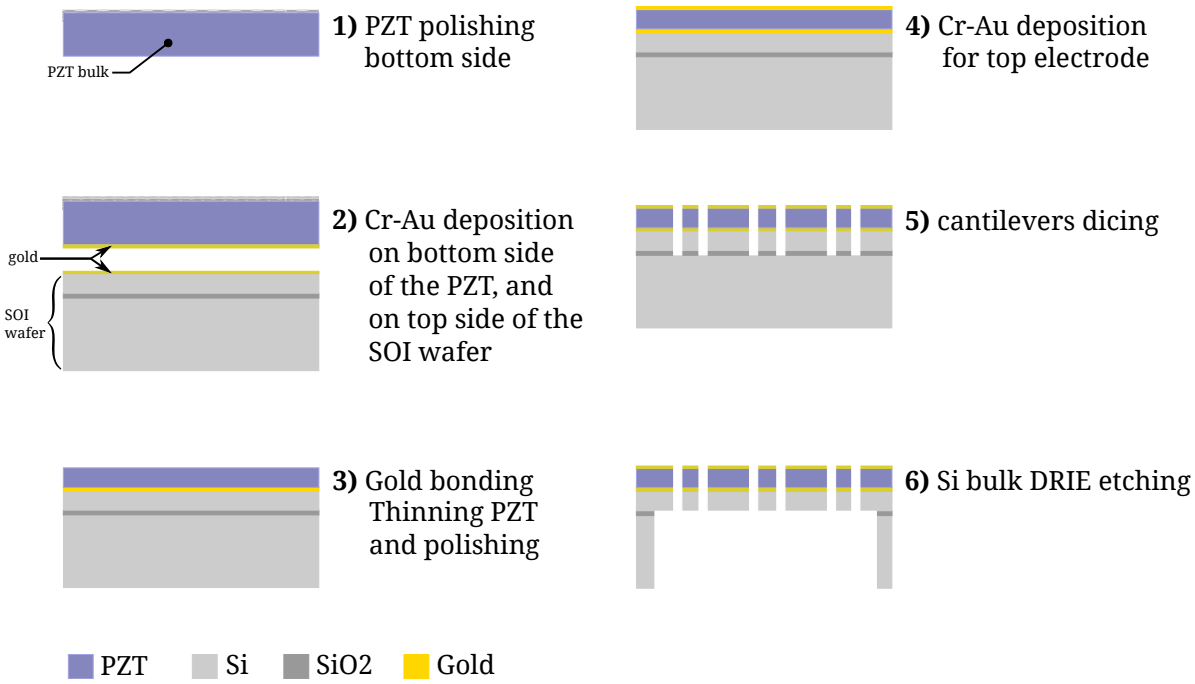

Figure 3: Flowchart of unimorph piezoelectric cantilevers fabrication.

with a hydraulic press. Mechanical thinning of the PZT layer can then be done with a solution of 9 µm aluminium oxide particle. Once thinned and polished, a top electrode of Cr-Au is deposited (step **4**) on top of the PZT layer to create the second electrode. Dicing of the cantilevers is done within step **5** with a saw, and finally released by dry etching through DRIE (step **6**) of the SOI handle layer. Figure 4 depicts one group of the fabricated cantilevers, corresponding to the set Long_3 of Table 2. A profile view of the wafer after gold bonding (step **3**) is shown in Figure 4(b).

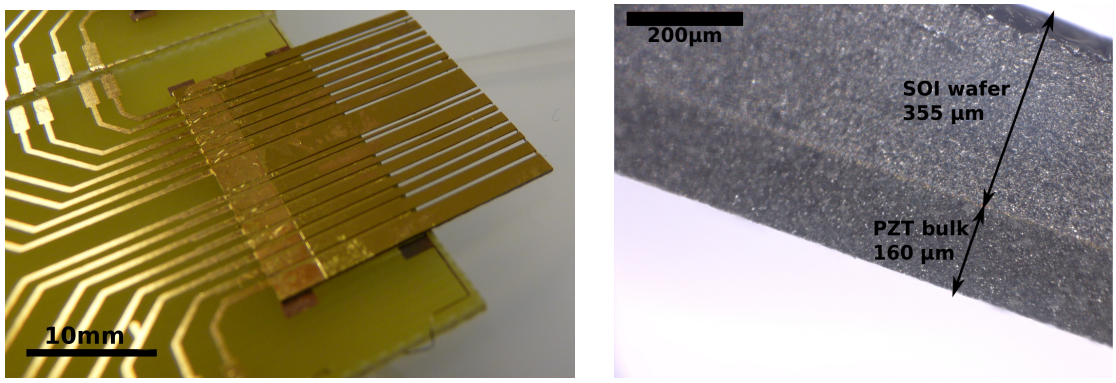

(a) (a) (b) (b)

Figure 4: The microfabricated cantilevers. (a) multiple cantilevers from the set Long_3. (b) a microscopic view of the wafer's profile after gold bonding (microfabrication step 3).

4. Experimental performances quantification

In order to characterize the static performances, a sine input voltage was applied at low frequency (0.1 Hz) with different amplitudes. The bending at the tip of each cantilever is recorded with an optical displacement sensor (laser sensor from *Keyence* company, with 200 µm range, 10 nm resolution). Figure 5 shows the bending displacement obtained with the Short_3 cantilever (48 µm PZT and 5 µm Si) for different driving voltage amplitudes (from $5V$ to $40V$). We particularly notice the gain of about $\frac{64\,\mu m}{40\,V} \approx 1.6\,\mu m\,V^{-1}$ of the fabricated cantilevers which is about twice the gain of existing bulk cantilevers (between $0.6\,\mu m\,V^{-1}$ and $1\,\mu m\,V^{-1}$) [28]. This figure shows the hysteresis behavior of the cantilever, which is a typical property of PZT ceramics.

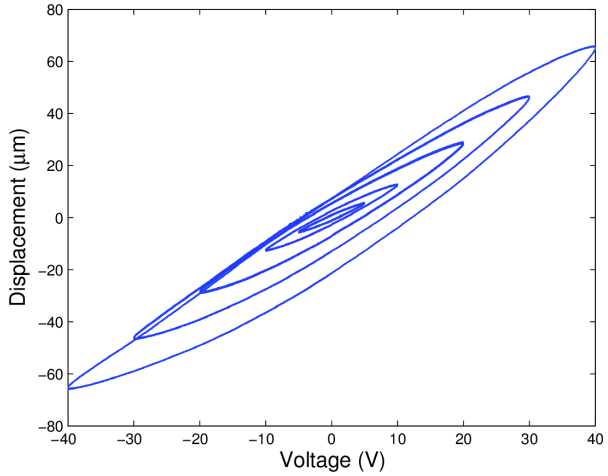

Figure 5: Experimental voltage / displacement relationship for the cantilever Short_3 (48 µm PZT and 5 µm Si) when sine input voltage is applied at different amplitudes (5 V, 10 V, 20 V, 30 V, 40 V).

Figure 6 shows the gain by thinning the PZT layer on the bending displacement. For each experimental result, simulation results using Eq. 1 is also given (dashed lines). Results with the long cantilevers (50 µm Si layer) are shown in Figure 6(a) while results with the short cantilevers are shown in Figure 6(b). These figures demonstrate that it is possible to reach the same bending displacement with a short cantilever as with a long cantilever, compare for instance the cantilevers Long_2 and Short_1. Short_1 is almost eight times thinner and more than twice as short as Long_2, however it only requires $\frac{1}{8}$ of the input voltage of Long_2 to reach a similar displacement value. Choosing an appropriate design will therefore allow to reduce the sizes of an actuator and to reduce its energy consumption while preserving or even increasing its performance. This can lead to important size reduction of microsystems while simultaneously increasing their capability.

Finally the experimental results are reported in the same graph displaying the displacement/voltage ratio versus the thickness of the piezoelectric layer. Figure 7 shows the theoretical simulation (solid lines) corresponding to the fabricated set of cantilevers

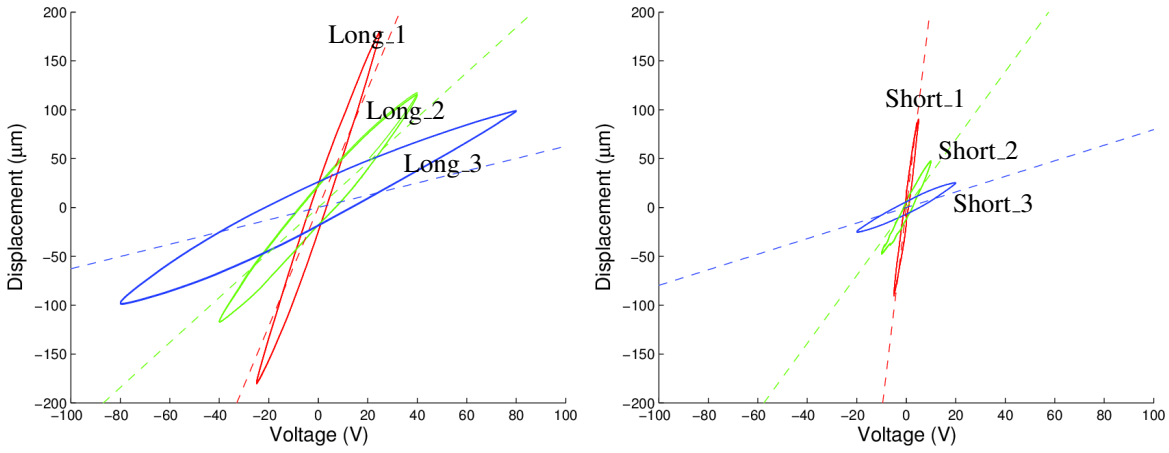

(a) (a) (b) (b)

Figure 6: Experimental results showing the bending displacement generated by different cantilevers and the comparison with simulation results (dashed lines from Eq. 1). (a) performances of the long cantilevers. (b) performances of the short cantilevers.

Table 3: Experimental performances of the different cantilevers

	Displacement / input voltage		Resonance frequency	
Cantilever	Experimental ($\mu m/V$)	Theoretical ($\mu m/V$)	Experimental (Hz)	Theoretical (Hz)
Short_1	18.0	21.0	535	609
Short_2	4.80	3.47	1103	1078
Short_3	1.25	0.80	1772	1733
Long_1	7.20	6.07	743	623
Long_2	2.93	2.30	944	820
Long_3	1.23	0.62	1305	1230

and the related experimental results (dots). We also report the resonance frequency of the cantilevers versus the thickness. Figure 8 depicts such resonance frequency where both the theoretical prediction (based on the model in Eq. 1 and Eq. 2) and the experimental results are plotted. The performances of these cantilevers are summarized in Table 3. These results can be compared with the standard behavior from literature, such as in [28, 30] which used 12 mm length cantilevers with 200 µm thickness PZT layer and 100 µm thickness copper as passive layer. These existing cantilevers generate a displacement of $0.67\,\mu m/V$ and exhibit a resonance frequency of $716\,Hz$.

5. Analysis and discussion

According to these characterizations, the static and dynamic behaviors of the fabricated cantilevers fit very well with the theoretical model described in [27]. This means that the

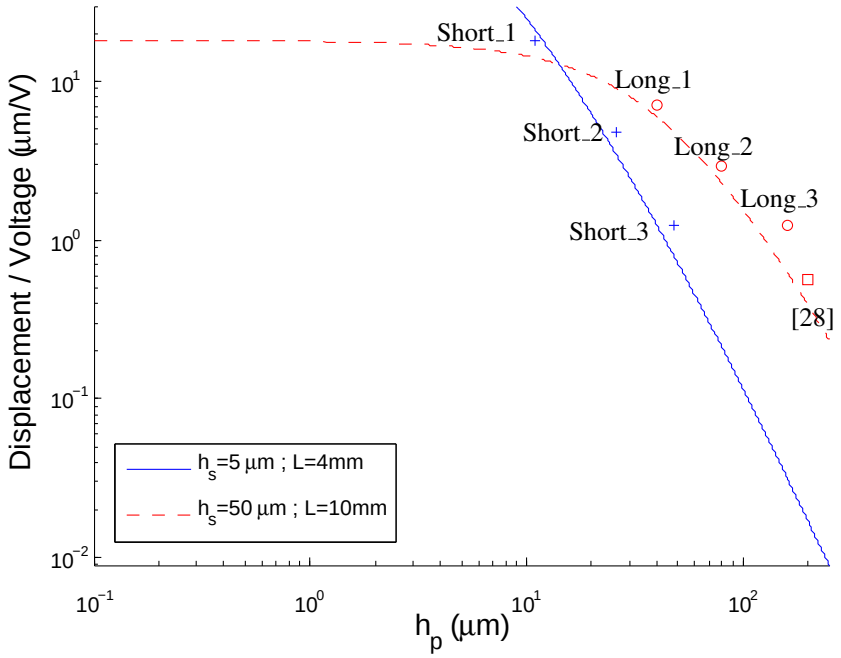

Figure 7: Displacement / Voltage ratio measured from experiments (cross and circle) of all the fabricated cantilevers. They are compared with the simulation results from Eq. 1 (solid and dashed lines). Compared to the results using a bulk PZT layer in [28].

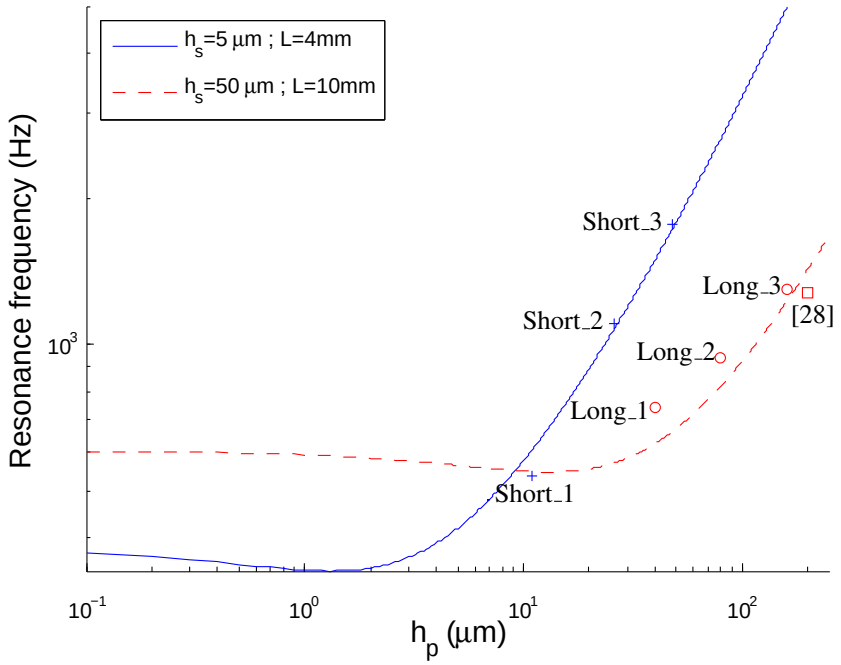

Figure 8: Resonance frequency measured from experiments (cross and circle), compared with the simulation results from Eq. 2 (solid and dashed lines). Compared to the results using a bulk PZT layer in [28].

developed actuators with the new process of microfabrication can still be described with the theoretical model which has been admitted to be precise for bulk piezoelectric materials only. In other words, the bulk properties have not been decreased or lost with the room temperature bonding. The figures also show that thinning the PZT layer substantially contributes to increase the generated displacement in general, even if the thickness of the silicon and the length of the cantilever also affect the performances. However, the resonance frequency decreases with the reduction of the PZT thickness (h_p).

The relationship between the resonance frequency and the displacement to voltage ratio is displayed in Figure 9 for all the fabricated cantilevers. It is compared with the standard values theoretically obtained for both thin film and bulk PZT fabrication processes (calculated with Eq. 1 and 2). As from the figure, we fill the gap between the standard fabricated cantilevers, which results in very good performances compromise both in static and dynamic aspects.

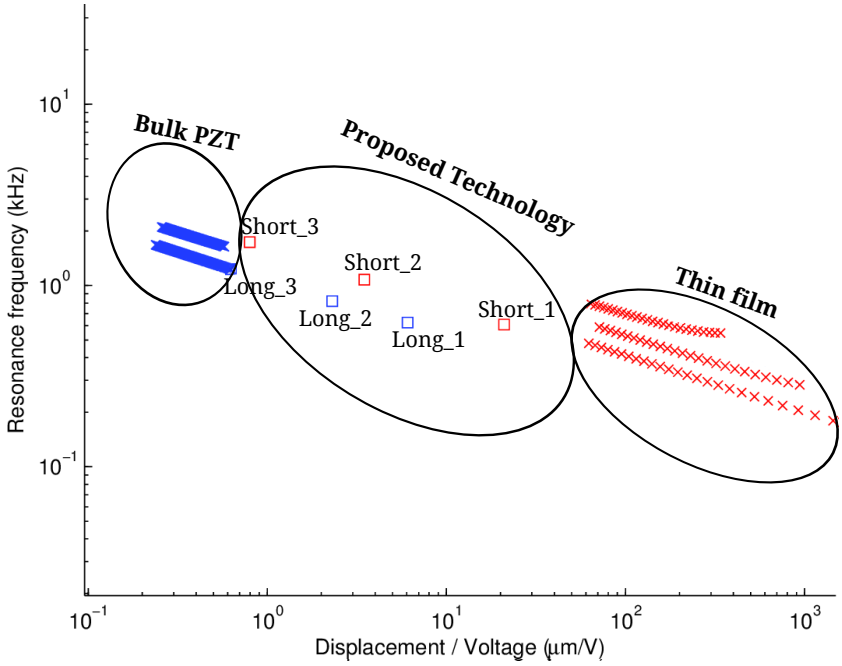

Figure 9: Performances of different unimorph cantilever designs. The squares are the measurements from the cantilevers fabricated in this study. They are compared with simulation results (from Eq. 1 and 2) for bulk PZT and thin film fabrication.

Table 4 summarizes the comparison between the three fabrication techniques. Thin film growth focuses on the fabrication of small cantilevers (small length and thickness) for which low energy consumption can be performed with a high generated displacement. On the contrary, bulk PZT layers imply larger structures and need higher voltages to finally generate lower displacements. However unlike thin films, bulk layers permit to have piezoelectric cantilevers with high resonant frequency. The technology proposed here allows a better flexibility by inheriting the advantages of these two technologies: large range of displacement, high bandwidth, small sizes, and low voltage. This is particularly obtained by employing bulk layers, gold-bonding them at low temperature onto silicon layers and thinning them.

Table 4: Comparison of the 3 techniques for fabrication of piezoelectric cantilevers.

	Thin film	Bulk PZT	Thick film
Piezoelectric layer thickness	0 to 5 µm	$> 160\,\mu m$	5 to 150 µm
Cantilever's length	$< 1\,mm$	$> 10\,mm$	few millimeters
Maximal voltage range	$< 10\,V$	$150\,V < x < 1\,kV$	$10\,V < x < 150\,V$
Generated displacement	$> 50\,\mu m\,V^{-1}$	$< 1\,\mu m\,V^{-1}$	$1\,\mu m\,V^{-1} < \delta < 50\,\mu m\,V^{-1}$
Bandwidth	few 100 Hz	$> 1\,kHz$	$0.5\,kHz < f_r < 2\,kHz$

The dimensions targeted by the proposed technology of microfabrication permits a better integration of high performances cantilever structures in microsystems.

Time consumption can also be an other element of comparison. The bonding process presented in this paper can be done very rapidly because neither heating nor slow cooling are required for the bonding process.

6. Conclusion and future works

This paper proposes a new range of piezoelectric actuators size and performances for integration inside complex MEMS. Based on the thinning of piezoelectric bulk material at low temperature, the process permit to maintain the bulk properties such as high stiffness, high bandwidth and benefits from the advantages of thin films piezoelectric such as very high displacement to voltage ratio and small sizes. Several cantilevers of different sizes have been fabricated and tested. The experimental characterization demonstrates the predicted advantages. With such cantilevers, the panel of displacement and frequency is enlarged compared to the existing dimensions. It becomes easier to choose the appropriate dimensions for a specific application. For instance performances from $1.2\,\mu m/V$ with a $1700\,Hz$ resonance frequency, up to $18\,\mu m/V$ with a $600\,Hz$ resonance frequency can be reached.

To demonstrate the advantage of such miniaturized cantilevers, the development of more complex structures is currently undergoing. The combination of the proposed bonding process and dry etching of the PZT layer (as used in [31]) will be used to create a 3DOF Cartesian platform. Future work includes therefore the utilization of the process to develop more complex piezoelectric structures in order to go towards high performances 3D MEMS with spatial integration of actuators.

Acknowledgments

These works were supported by the national project ANR-11-EMMA-006 (MYMESYS) and the national ANR-JCJC C-MUMS-project (National young investigator project ANR-12- JS03007.01: Control of Multivariable Piezoelectric Microsystems with Minimization of Sensors). These works have also been partially supported by the Franche-Comté region and the OSEO, by the Labex ACTION project (contract ANR-11-LABX-01-01) and by the

French RENATECH network through its FEMTO-ST technological facility. We would like to acknowledge David Guibert for his technical support.

References

[1] Janphuang P., Lockhart R., Uffer N., Braind D. and de Rooij N.F. (2014). Vibrational piezoelectric energy harvesters based on thinned bulk PZT sheets fabricated at the wafer level. *Sensors and Actuators A: Physical*, **210**, pp. 1-9.

[2] Lafitte N., Haddab Y., Le Gorrec Y., Guillou H., Kumemura, M., Jalabert L., Collard D. and Fujita H. (2013). Active control of silicon nanotweezers detects enzymatic reaction at the molecular level. *The 17th International Conference on Transducers & Eurosensors XXVII*, pp 2357-2360.

[3] Aljasem K., Froehly L., Seifert A. and Zappe H. (2011). Scanning and tunable micro-optics for endoscopic optical coherence tomography, *Journal of Microelectromechanical Systems*, **20**(6), pp. 1462-1472.

[4] Bargiel S., Rabenorosoa K., Clévy C., Gorecki C. and Lutz P. (2010). Towards micro-assembly of hybrid MOEMS components on a reconfigurable silicon free-space micro-optical bench. *Journal of Micromechanics and Microengineering*, **20**(4), 045012.

[5] Chalvet V., Haddab Y. and Lutz P. (2013). A microfabricated planar digital microrobot for precise positioning based on bistable modules. *IEEE Transactions on Robotics*, **29**(3), pp. 641-649.

[6] Liu X., Kim K. and Sun Y. (2007). A MEMS stage for 3-axis nanopositioning. *Journal of Micromechanics and Microengineering*, **17**(9), pp. 1796.

[7] Rakotondrabe M., Ivan I. A., Khadraoui S., Clévy C., Lutz P. and Chaillet N. (2010). Dynamic displacement self-sensing and robust control of cantilever piezoelectric actuators dedicated for microassembly. *IEEE/ASME International Conference on Advanced Intelligent Mechatronics*, pp. 557-562.

[8] Binnig G. and Rohrer H., (1986). The scanning tunneling microscope. *Scientic American*, **253**, pp. 5056.

[9] Agnus J., Chaillet N., Clévy C., Dembélé S., Gauthier M., Haddab Y., Laurent G., Lutz P., Piat N., Rabenorosoa K., Rakotondrabe M. and Tamadazte B., (2013). Robotic Microassembly and micromanipulation at FEMTO-ST. *Journal of Micro-Bio Robotics (JMBR)*, **8**(2), pp. 91-106.

[10] Liao W., Liu .W, Zhu Y., Tang Y., Wang B., and Xi H., (2013). A Tip-Tilt-Piston Micromirror With Symmetrical Lateral-Shift-Free Piezoelectric Actuators. *IEEE Sensors Journal*, **13**(8), pp. 2873-2881.

[11] Fadel L., Lochon F., Dufour I. and Français O. (2004). Chemical sensing: millimeter size resonant microcantilever performance. *Journal of Micromechanics and Microengineering*, **14**, pp. S23-S30.

[12] Fu L., Li S. Zhang K. Chen I.H., Barbaree J.M., Zhang A. and Cheng Z., (2011). Detection of Bacillus anthracis Spores Using Phage-Immobilized Magnetostrictive Milli/Micro Cantilevers. *IEEE Sensors Journal*, **11**(8), pp. 1684-1691.

[13] Johnson B. N. and Mutharasan R. (2013) A cantilever biosensor-based array for toxin-producing cyanobacteria microcystis aeruginosa using 15S rRNA *Environmental Science & Technology*, pp. 12333-12341.

[14] Johnson B. N. and Mutharasan R. (2012) Sample preparation-free, real-time detection of microRNA in human serum using piezoelectric cantilever biosensors at attomole level. *Analytical chemistry*, pp. 10426-10436.

[15] Ziegler C. (2004). Cantilever-based biosensors. *Analytical and bioanalytical chemistry*, **379**, pp. 946-959.

[16] Lavrik N. V., Sepaniak M. J. and Datskos P. G. (2004) Cantilever transducers as a platform for chemical and biological sensors. *Review of scientific instruments*, pp. 2229-2253.

[17] Johnson B. N. and Mutharasan R. (2012) Biosensing applications using dynamic-mode cantilever sensors: a review. *Biosensors and bioelectronics*, **32**(1), pp. 1-18.

[18] Komati B., Agnus J., Clévy C. and Lutz P. (2014) Prototyping of a highly performant and intregrated piezoresistive force sensor for microscale applications. *Journal of Micromechanics and Microengineering*, **24**, pp. 035018.

[19] Kanno I., Kotera H. and Wasa K. (2003). Measurement of transverse piezoelectric properties of PZT thin films. *Sensors and Actuators A: Physical*, **107**(1), pp. 68-74.

[20] Wang Z., Miao J., Tan C. and Xu T. (2010). Fabrication of piezoelectric MEMS devices-from thin film to bulk PZT wafer. *Journal of Electroceramics, Springer US*, **24**, pp. 25-32.

[21] Xu X. H., Li B. Q., Feng Y., and Chu J. R. (2007). Design, fabrication and characterization of a bulk-PZT-actuated MEMS deformable mirror. *Journal of Micromechanics and Microengineering*, **17**(12), pp. 2439.

[22] Yi-Gui L., Jian S., Chun-Sheng Y., Jing-Quan L., Susumu S. and Katsuhiko T. (2011). Fabrication and characterization of a lead zirconate titanate micro energy harvester based on eutectic bonding. *Chinese Physics Letters* **28**(6), pp. 068103.

[23] Wilson S. A., Jourdain R. and Owens S. (2009). Pre-stressed piezoelectric bimorph micro-actuators based on machined 40 μm PZT thick films: batch scale fabrication and integration with MEMS *ASME 2009 Conference on Smart Materials, Adaptive Structures and Intelligent Systems*. pp. 247-252.

[24] Tanaka K., Konishi T., Ide M., Meng Z. and Sugiyama S. (2005). Fabrication of microdevices using bulk ceramics of lead zirconate titanate. *Japanese Journal of Applied Physics*. **44**(9S), pp. 7068.

[25] Wang Z., Miao J. and Tan C. W. (2009). Acoustic transducers with a perforated damping backplate based on PZT/silicon wafer bonding technique. *Sensors and Actuators A: Physical* , **149**, pp. 277-283

[26] Aktakka E. E., Peterson R. L. and Najafi K. (2013). A 3-DOF piezoelectric micro vibratory stage based on bulk-PZT/silicon crab-leg suspensions. *IEEE 26th International Conference on Micro Electro Mechanical Systems*, pp. 576-579.

[27] Ballas R.G.(2007). Piezoelectric multilayer beam bending actuators : Static and dynamic behavior and aspects of sensor integration. *Springer*.

[28] Ivan I.A., Rakotondrabe M., Agnus J., Bourquin R., Chaillet N., Lutz P., Ponçot J.-C., Duffait R., Bauer O., (2010). Comparative material study between PZT ceramic and newer crystalline PMN-PT and PZN-PT materials for composite bimorph actuators. *Review on Advanced Materials Science (RAMS)*, **24**(1), pp. 1-9.

[29] Bassignot F., Courjon E., Ulliac G., Ballandras S., Lesage J-M. and Petit R. (2012). Acoustic resonator based on periodically poled transducers: Fabrication and characterization. *Journal of Applied Physics*. **112**(7), pp. 74108.

[30] Rakotondrabe M., Haddab Y. and Lutz P., (2009). Quadrilateral modelling and robust control of a nonlinear piezoelectric cantilever. *IEEE Transactions on Control Systems Technology (T-CST)*, **17**(3), pp 528-539.

[31] Aktakka E. E., Peterson R. L. and Najafi K. (2013) A 6-DOF piezoelectric micro vibratory stage based on multi-axis distributed-electrode excitation of PZT/Si unimorph T-beams. *IEEE International Conference on Solid-State Sensors, Actuators and Microsystems*, pp. 1583-1586